Journal of Physics: Conference Series **488** (2014) 012019 doi:10.1088/1742-6596/488/1/012019

An extreme ultraviolet interferometer using high order harmonic generation

D E Laban[1,2], A J Palmer[1,2], W C Wallace[1,2], N S Gaffney[1,2], R P M J W Notermans[1,2], T T J Clevis[1,2], M G Pullen[1,2], D Jiang[3], H M Quiney[3], I V Litvinyuk[1,2], D Kielpinski[1,2] and R T Sang[1,2] †

[1] Australian Attosecond Science Facility and Centre for Quantum Dynamics, Griffith University, Nathan, QLD, 4111, Australia
[2] ARC Centre of Excellence for Coherent X-Ray Science, Griffith University, Nathan, QLD, 4111, Australia
[3]ARC Centre of Excellence for Coherent X-Ray Science, University of Melbourne, Melbourne, Victoria 3010, Australia

E-mail: r.sang@griffith.edu.au

Abstract. We present a new interferometer technique based on the interference of high-order harmonic generation radiation from translatable successive gas jets. The phase shifts in the apparatus are shown to originate from the Gouy phase shift of the driving laser. The technique can be used to deliver time delays between light pulses and we demonstrate the unprecedented capability of delivering pulses of extreme ultraviolet light delayed in time by as small as 100 zeptoseconds.

1. Introduction

The use of ultrafast pulsed lasers with high intensities has allowed nonlinear optical phenomena to be investigated. One of these phenomena is high-order harmonic generation (HHG). HHG is the process where an atom is exposed to a time-varying electric field in which the field strength approaches the outer electron's Coulomb binding energy and causes it to be tunnel-ionised. The now free electron is then accelerated in the electric field and recombines with the parent ion to emit a photon. As the ionised electron is accelerated in the field, the energy of the photon produced will be equal to the energy of the returning electron plus the first ionisation energy of the atom. Typically, photon energies extend into the extreme ultraviolet (XUV) region. As the electric field is periodic, the emitted photon spectrum will show odd harmonics of the driving laser frequency [1, 2]. The time that the electron is ionised in the electric field plays an important role in determining the trajectory and energy of the electron. Figure 1 depicts two trajectories of ionised electrons as they are accelerated by the electric field. The blue trajectory is an electron that has been ionised earlier in the electric field than the green trajectory. As such, the blue trajectory does not re-encounter the parent ion whereas the green trajectory may result in the emission of a HHG photon. The HHG process is coherent and all the photons emitted are in phase. A lot of research has been performed to maximise the radiation yield through quasi-phase-matching schemes [3] and the use of multiple gas jet arrays [4]. Seres et al found that the yield of two successive generation sources within a single laser focus depended on the separation of the sources [5]. At a particular separation a coherent superposition of the radiation generated from each source was found and the radiation yield was greater than when the sources were

placed beside one another. Although the physical mechanism responsible for the quasi-phase matching of the yield at certain separations was not revealed by their measurements. The authors concluded that the observed coherent separation was too large to be from the Gouy phase of the driving laser alone.

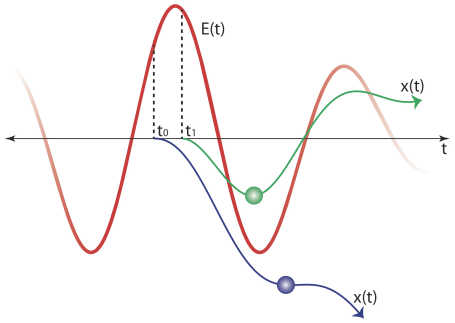

Figure 1. Two electron trajectories with different ionisation times in the electric field. The trajectory originating at t_0 results in the electron not recombining with the parent ion. Whereas the trajectory originating at t_1 returns to the vicinity of the nucleus and may result in a HHG photon being emitted.

One of the many uses of HHG radiation is in the emerging field of attosecond science. The emitted HHG radiation consists of a pulse train separated by half the period of the driving laser, with each pulse having a duration in the order of attoseconds. There are several methods that can be used to isolate a single attosecond pulse from the pulse train [1]. The duration of an isolated attosecond pulse created from a carrier-envelope phase stabilised few-cycle driving laser have been as short as 80 attoseconds [6]. The duration of these attosecond pulses routinely approaches or are shorter than the Bohr orbit time of an electron in a hydrogen atom, approximately 150 as, making it possible to directly observe electron motion for the first time [7, 8]. One difficulty encountered when working with short-wavelength radiation is that it is technically challenging to impart small time delays between multiple pulses with current interferometric techniques. As current techniques used for visible light involve delaying pulses using bounces on mirrors, the mirror surface has to be stabilised to a fraction of the wavelength. The best resolution currently available is 20 attoseconds in a Mach-Zehnder interferometer with a co-propagating 532 nm reference laser used to provide stabilization feedback [9]. Other experiments utilising active pulse shaping techniques with feedback stabilisation have demonstrated the ability to precisely delay two 10 fs, 800 nm pulses down to 280 zs [10]. However, this method cannot be employed for XUV radiation or for delays within the timeframe of half of the period of the driving laser.

In this paper, we demonstrate that the Gouy phase shift of the driving laser can be utilised to impart a small time delay on the ionised electron recombining with the parent ion in the HHG process between two successive sources. This then causes a corresponding time delay between the attosecond pulse trains generated at each source. In this manner, a time delay is engineered between two XUV emissions by altering the separation of two generation sources along the propagation length of a single few-cycle infrared laser pulse's focus. This allows for time delays within one half of the driving laser's period to be created, something not possible with current interferometric techniques. The resolution of the time delay is investigated and found to be better than 100 zeptoseconds. This work has been previously reported [11] and in this paper a heavier focus is placed on the experimental apparatus used to produce the result to complement the original publication.

2. XUV interferometer apparatus

The apparatus that is used to produce the time delayed XUV pulses is shown in figure 2. The driving laser is a commercially available Femtolaser Femtopower Compact Pro that produces sub-5.6 fs pulses

centered at 800 nm at a repetition rate of 1 kHz and energy of 200 μJ using titanium:sapphire as the gain media. It consists of four sections: the oscillator and stretcher, amplifier, prism compressor, and the hollow core fiber compressor and double-chirped mirror (DCM) set. An interferometric autocorrelator and spectrometer (not pictured in the diagram) are used to measure the pulse duration and bandwidth of the driving laser, respectively. An off-axis parabolic (OAP) mirror is used to focus the driving laser into the experiment chamber. The OAP mirror has a focal length of 750 mm and an off-angle distance of 130 mm. This mirror is used to minimise any spherical aberration or astigmatism at the focus that would result if a spherical mirror were used in an off-axis configuration. The total beam path length from the end of the DCM set to the OAP mirror is approximately 10m. The entire apparatus is mounted onto an optical table that is pneumatically isolated from the ground to minimise any vibration noise coupling into the laser.

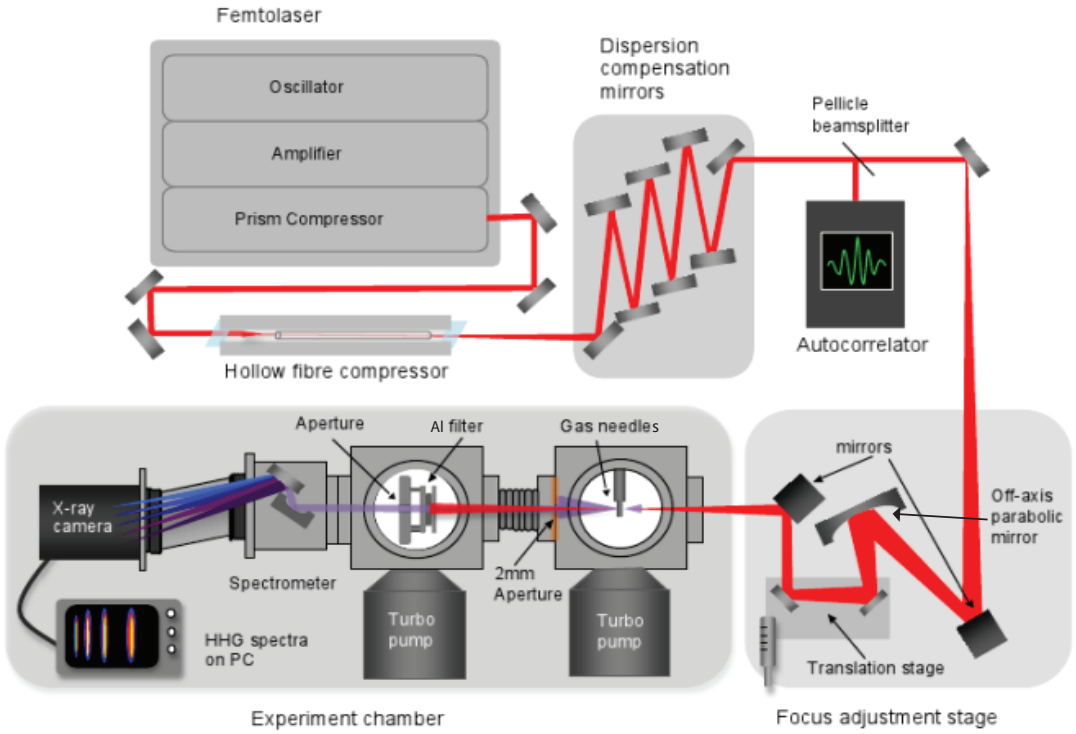

Figure 2. Layout of the XUV interferometer apparatus. The second gas needle in the experiment chamber cannot be seen as it is pointing directly up and out of the page.

The experiment chambers are constructed of stainless steel with Conflat flanges to maintain a good vacuum when running experiments. The first chamber is the generation section where two gas needles are located. These act as the source of atoms for the HHG process and are made from 250 μm hypodermic syringes with blunted tips. The driving laser is focused just above the tips of the gas needles and the estimated interaction length of the laser and the gas is 400 μm. For the experiments in this paper, argon was used in the gas needles at a backing pressure of 100 Torr. More details of the mounting of the gas needles is given in the next paragraph. A turbo pump with a pumping speed of 550 L/s is used in the generation chamber and typically the background operating pressure reaches experiment 10 mTorr. The next section is the filter chamber which houses a thin metal foil to filter out the driving laser and allow the XUV to pass through. We use a dual layer aluminium foil with each layer consisting of 100 nm. When a single layer of foil is produced it contains pinholes that allow the driving laser to leak through and combining two layers reduces IR light leakage by many orders of

magnitude. A 250 L/s turbo pump is used on the filter chamber and a 2mm vacuum aperture is located between the filter and generation chambers to allow a typical operating pressure of 10^{-6} Torr. The final section is the spectrometer and camera that are used to resolve the HHG spectrum. The spectrometer is a commercially available Hettrick Scientific grazing incidence model and the spectrum is digitised with a PI XUV CCD 2048x512 array.

The gas needles are mounted perpendicular to one another in the generation chamber as this was found to give the least amount of cross talk on the gauges measuring the backing pressures. One gas needle is statically mounted on the base of the chamber and is pointing upwards. The other is mounted from the side on a piece of vacuum bellows such that it can be translated along the propagation direction of the laser from the outside of the chamber. This configuration gives one stationary gas needle in the center of the chamber and another that can be translated away from the stationary one. The procedure for aligning the driving laser is to peak the HHG yield that is generated from the stationary gas needle, thus ensuring it is at the focus. The translatable gas needle is then moved into position beside the stationary needle. This method was found to be highly reproducible in our experiments.

3. XUV interferometer operating theory

The Lewenstein model for HHG gives the phase of the emitted radiation as the following [12, 13],

$$\phi = q\omega t_{\mathrm{r}} - \frac{1}{\hbar} S(p_{\mathrm{st}}, t_{\mathrm{i}}, t_{\mathrm{r}}) \tag{1}$$

where q is the harmonic number, ω is the angular frequency of the driving laser, t_r is the return time of the ionised electron, and S is the semi-classical action of the electron as it travels in the electric field. The semi-classical term is dependent on the intensity of the electric field as well as the travel time of the electron in the field. Near the center of a laser focus, neither the intensity nor the travel time changes substantially. However, there is another effect that will result in the return time of the electron being altered near the center of the focus and that is the Gouy phase. The Gouy phase describes a π phase shift of a Gaussian laser beam as it passes through a focus [14] and it has been experimentally observed to produce a shift in the carrier-envelope phase (CEP) of few-cycle pulses [15]. The Gouy phase accumulated along the propagation length of the laser is,

$$\phi_{\mathrm{Gouy}}(z) = -\arctan\left(\frac{z}{z_{\mathrm{R}}}\right) \tag{2}$$

where z is the propagation length away from the focus and z_R is the Rayleigh range of the focus. It is predicted that as the Gouy phase alters the CEP of the driving laser, and in turn the electron recombination time will be altered by a corresponding amount. This is due to the ionisation time and trajectory of the electron that gives rise to a certain energy photon also being shifted in time relative to the envelope of the driving laser pulse. The peak of the envelope of the driving laser is used as to define the time axis, as the group velocity does not change within the focus, only the phase velocity is affected. Figure 3 depicts the operating principle of the XUV interferometer.

A first order theory can be used to test the hypothesis that the Gouy phase will cause a delay in the electron recombination time between two HHG sources separated by some distance Δz. More details of this can be found in our original publication [11]. If this theory is correct then the coherent revival position z_c, i.e. the separation that gives a coherent superposition of the XUV generated in each source, should follow the equation,

$$z_{\mathrm{c}} = 2\pi\left[q\frac{d\phi_{\mathrm{Gouy}}}{dz} + \frac{d\phi_{\tau,S}}{dz}\right]^{-1} \tag{3}$$

where the first derivative term is related to the Gouy phase shift and the second is the phase shift due to the action and travel time of the electron. If the experiment is carried out near the centre of the focus, the Gouy phase term will dominate and the other term will be approximately zero.

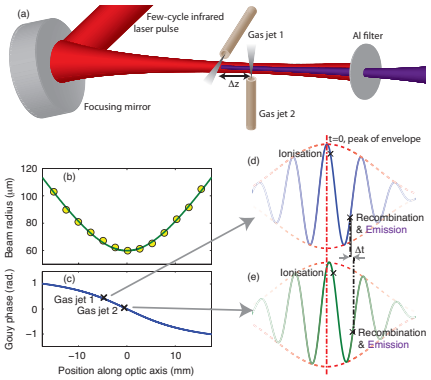

Figure 3. The Gouy phase of the laser (c) causes a shift in the electron recombination and photon emission time (d) and (e).

4. Results

The experiment results for the XUV interferometer are shown in figure 4 and figure 5. Figure 4 shows the constructive and destructive interference observed in the harmonics as the gas jet separation is increased. Figure 5 has the inverse revival distance (z_c^{-1}) plotted against the harmonic order (q). In this plot, equation (3) has been used to fit the red line. The fit gives the derivate of the Gouy phase shift and action-phase term. The derivative of the Gouy phase shift was used to calculate a Rayleigh range of 12.4±2.3 mm and this compares well with the value measured from beam profiling of 10.9±0.5 mm. While the action phase term came to be −78±62 rad/m, which is consistent with the prediction of 0 near the center of the focus. These results confirm the hypothesis that the Gouy phase introduces a time delay between the emissions from each gas jet.

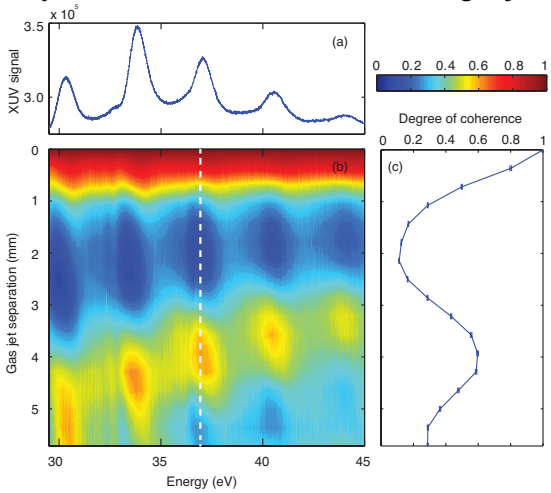

Figure 4. (a) shows the HHG spectrum of 5 harmonics. (b) is the data showing the constructive and destructive interference as the gas jet separation is increased. (c) is the degree of coherence data for the dashed line in (b). The degree of coherence calculation can be found in our original publication [11].

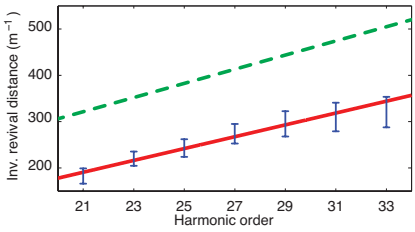

Figure 5. The inverse coherent revival data (errorbars). The solid line is a fit to the data using equation (3). The dashed line is only the Gouy phase term as calculated from the beam profiled Rayleigh range.

In the original publication, the resolution of the imparted time delay was explored by using an Allan variance measurement shown here in figure 6 [11]. It was found that the timing resolution could be better than 100 zs, an unprecedented measurement in stability from an interferometer-like device.

This stability comes from the fact that any vibration in the apparatus has to be compared relative to the Rayleigh range of the laser focus, as opposed to more traditional interferometers where the vibration is compared to the wavelength of the radiation. To illustrate this point, a simplified theory whereby the Gouy phase is wholly responsible for the delay can be used and an equation can be derived to show how the timing resolution is affected by vibration,

$$\Delta t \approx \frac{\Delta z_{\mathrm{vibration}}}{\omega z_{\mathrm{R}}} \tag{4}$$

where Δt is the expected time resolution if there is a vibration of $\Delta z_{vibration}$ on, for example, the gas needles. For our passive experiment that doesn't involve any stabilisation $\omega \approx 2.4\times10^{15}$ rad/s, $z_R \approx 11$ mm, and $\Delta t \approx 100$ zs. This implies that the gas needles are vibrating by approximately 3 μm, which is quite large when compared to traditional interferometers with stabilised mirrors. If the gas needles were actively stabilised, it is possible that better timing resolutions of the XUV interferometer could be achieved.

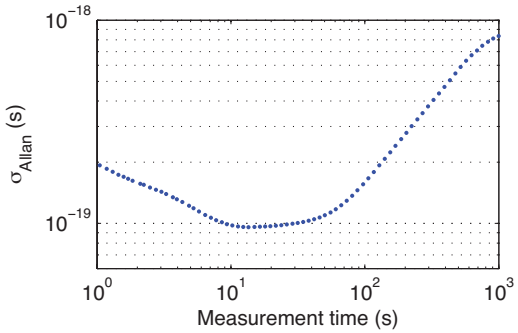

Figure 6. The Allan variance of the XUV interferometer. Between 8 and 30 seconds of measurement time, a timing resolution of less than 100 zeptoseconds is achieved.

5. Conclusion

The XUV interferometer demonstrates an unprecedented ability to produce pairs of XUV pulse trains with an accurate time delay between them. The apparatus uses two successive sources that are located within a single driving laser focus. The mechanism that causes the time delay has been shown with a first order theory to be predominantly the Gouy phase near the laser focus. This apparatus has potential practical use in the field of attosecond science and allows for future experiments using XUV as the pump and probe to be accomplished.

References

[1] Corkum P & Krausz F, Nature Physics 3, 381–387 (2007).
[2] Krausz F. & Ivanov M, Reviews of Modern Physics 81, 163–234 (2009).
[3] Paul A et al., Nature 421, 51–54 (2003).
[4] Willner A et al., Physical Review Letters 107, 175002 (2011).
[5] Seres J et al., Nature Physics 3, 878–883 (2007).
[6] Goulielmakis E et al., Science 320, 1614–1617 (2008).
[7] Worner H, Bertrand J, Kartashov D, Corkum P & Villeneuve D, Nature 466, 604–607 (2010).
[8] Goulielmakis E et al., Nature 466, 739–743 (2010).
[9] Chini M et al., Optics Express 17, 21459-21464 (2009).
[10] Kohler J et al., Optics Express 19, 11638–11653 (2011).
[11] Laban DE et al., Physical Review Letters 109, 263902 (2012).
[12] Balcou P, Salieres P, & L'Huillier A, Physical Review A 55, 3204–3210 (1997).
[13] Lewenstein M, Salires P, & L'Huillier A, Physical Review A 52, 4747–4754 (1995).
[14] Gouy LG, C. R. Acad. Sci. Paris 110, 1251 (1890).